Hindawi Publishing Corporation
International Journal of Antennas and Propagation
Volume 2013, Article ID 191685, 8 pages
http://dx.doi.org/10.1155/2013/191685

Research Article

The Design and Experiments on Corner Reflectors for Urban Ground Deformation Monitoring in Hong Kong

Yuxiao Qin, Daniele Perissin, and Ling Lei

Institute of Space and Earth Information Science, The Chinese University of Hong Kong, Hong Kong

Correspondence should be addressed to Yuxiao Qin; yuxiao@cuhk.edu.hk

Received 2 November 2012; Revised 23 December 2012; Accepted 5 January 2013

Academic Editor: Deren Li

PSInSAR technology has been proved to be a powerful tool for monitoring urban ground displacement information to a millimetric accuracy. When it comes to the validation of PS-derived ground deformation, artificial corner reflector (CR) can be very useful due to its relative stability and high signal-to-noise ratio (SNR). In this paper, we will evaluate some general criteria for designing and setting up corner reflectors, including the shape, size, material, location, and others. An ideal prototype known as the rectangular trihedral with special designs is brought up in this paper, and validation experiments were conducted in Hong Kong to demonstrate the ability of the proposed prototype. The field data agreed with theoretical analysis, bringing up an economical and applicable approach for CR application in urban ground deformation monitoring.

1. Introduction

In recent years, Interferometry Synthetic Aperture Radar (InSAR) [1, 2] technology has been proved to be a powerful tool that can provide high-resolution information on topography and ground displacement [3]. Furthermore, in order to overcome the limitations of InSAR technology, namely, the spatiotemporal decorrelation and atmospheric disturbance displacement [4–6], Permanent Scatterers (PSInSAR) technology [5, 6] was proposed. The technique can effectively identify, estimate, and remove atmospheric distortions, leaving the PS displacement as the only contribution to the signal phase shift, and it has been proved that 1 mm accuracy for deformation monitoring can be achieved [7]. Since then, the technology has been applied widely in ground displacement monitoring [8–10].

However, in practice, sometimes artificial scatterers are needed for PSInSAR measurement for various reasons. In the first place, PSInSAR-derived displacement is the relative movement to a reference point that usually possesses a high coherence and known displacement. Assuming that the entire region of monitoring area is descending, thus an artificial scatterer can be used as the reference point, and the deformation of scatterer can be usually precisely measured by other instruments. In the second place, when it comes to the validation of PSInSAR measurements, an artificial scatterer should be a preferred option to retrieve deformation trend, making them very useful for validation purpose. In general, artificial scatterers were manually lifted or lowered with millimetric precision and compared with the PSInSAR-derived results. As a consequence, corner reflector is brought up as one of the most commonly applied artificial scatterers. Corner reflectors are objects that exhibit a high radar cross-section (RCS) and a high signal-to-noise ratio (SNR). These typical characteristics of CR qualify it InSAR analysis.

In this paper, we will discuss the general principle for building a "user-friendly" corner reflector for InSAR analysis. A common rectangular trihedral reflector with a relative small size of 0.5 m wide basement and 0.75 m height, holed plate, and adjustable basement is proposed. The small size guarantees the mobility and stability of the reflector, while the adjustable basement makes it adjustable and more precise. In addition, under the premise of a reasonable RCS or at least a high SNR, the plates of CR are holed to withdraw the power of wind and filter the precipitation. The RCS and SNR are calculated to demonstrate the applicability of the proposed

CR. In the end, the performance of this kind of reflector is evaluated, and the result demonstrates that for regional subsidence validation, the proposed CR can achieve 1 mm stability.

2. Corner Reflector

2.1. General Criteria for Designing a Corner Reflector. In general, a corner reflector should be built regarding the following principles: it should be easy to point, light to carry, easy to mount, difficult to be reached by unauthorized people, well fixed, and resistant to all weather conditions. Additionally, in particular for a validation experiment, the height must be adjustable. To meet the above requirements, a prototype shown in Figures 1 and 2 is designed and assembled. This prototype possesses the following characteristics: first of all, it is in cubic shape and made of aluminum and the side panels are holed to reduce the weight. Secondly, the reflector is fixed onto a concrete basement on the ground with four anchors and screws to fix and adjust its height. The advantage of this type of corners is that it does not require any complicated pointing procedure and can be mounted easily. When deploying the CR, one simply turns the mouth to the satellite viewing direction. More detailed discussion of the reflector will be carried out in the following section.

2.2. The Material of Corner Reflector. For the reason of keeping the mechanical stability and accuracy of artificial shifts to a millimetric level, both the size and the weight of the structure should be kept limited. In this regard, the corner reflector in this case is made of aluminum, which is remarkable for its low density and ability to resist corrosion due to the phenomenon of passivation. The density of common aluminum alloy varies from 2.6 g/cm^3 to 2.9 g/cm^3, while the density of common iron and steel can vary from 7.75 to 8.05 g/cm^3. For example, a small trihedral corner reflector made of aluminum with a size of 50 cm $*$ 50 cm $*$ 75 cm and 2 mm width weighs approximately 5.6 kg (take density as 2.8 g/cm^3), but if the same corner is made of steel, it will weigh 16 kg (8 g/cm^3) in total, which is a remarkable increasing in weight.

2.3. The Shape of Corner Reflector. In principle, the reflector should be characterized by a reflectivity much higher than that of the surrounding scatterers [7]; that is to say, the reflector should have a high RCS for a relative small size. Some of the most common corner reflectors being used are flat plate, dihedral, triangular trihedral, and cubic trihedral, and their featured RCSs [11] are listed in Table 1. From the table, we can see that the circular trihedral offers the greatest RCS. However, considering the fact that the square trihedral offers a maximum RCS very close to that of circular ones, yet making square trihedral is easier than making circular ones, it is considered better to use rectangle trihedral in this case. In addition, although dihedral is favored for its lightness and simply design [12–15], we choose cubic trihedral for the following reasons. In the first place, the aluminum and holed plate can effectively reduce the weight of corners, overcoming the disadvantage of cumbersome compared with dihedral; in the second place, compared with the dihedral, the trihedral is more tolerant to the deviation of incident angles from the maximum angle, which suggests that trihedral would produce relatively large RCS even when the incident signal is not at the most ideal angle [16]. From these analyses, it seems that cubic trihedral corner reflector would serve as the best choice due to its robust geometric construction, relatively high tolerance of the incident signal's deviation from the optimal angle, and relatively high RCS value.

For TerraSAR-X satellite with wavelength $\lambda = 3.1$ cm and a small corner reflector with an edge of 0.5 m and height of 0.75 m, the maximum theoretical RCS $\sigma \approx 38.7$ dB; for a bigger reflector with edge of 1 m, the maximum theoretical RCS $\sigma \approx 48.6$ dB, both making it very easy to be identified from a low RCS background.

2.4. The Holed Plate. As stated above, the reflectors are exposed in open air and should be resistant to all weather conditions, mostly precipitation and wind. To solve the problem, the holed plates are introduced to the design of reflectors. With the holes on the plate, the wind forces will be lower, water can be filtered through the base, and the weight of the object can be reduced. For example, for the holed plate designed in Figure 3, for each plate, the holes can significantly reduce the weight by 35%.

However, the holed designation will result in a loss of RCS reflectance, and the transmittivity through holes can be calculated by the following formula [17]:

$$T_{db} = 20 \lg\left(\frac{3ab\lambda_0}{2\pi d^3 \cos\theta}\right) + \frac{32t}{d}, \quad (1)$$

where θ is the incidence angle and t is the plate thickness. a, b, and d are shown in Figure 3.

Typically, the dimension of the hole should be less than $\lambda/8$. However, considering that the incidence on the plates is never 0° and the different scattering properties at different frequencies, it can be demonstrated that in the case of C-band and X-band the holes on the plates can reach a diameter of 1 cm, with a respective filled/vacuum ratio of the plates of 60%, preserving a good RCS [18]. In this case, according to the diameter of holes, distance between holes, the wavelength of X-band (we will be using the reflector for TerraSAR-X calibrations), and the incidence angle (37° in this case) of TerraSAR-X satellite, we can calculate that the RCS loses $T_{dB} \approx 21$ dB. For the smaller reflector, the maximum RCS is 38.7 dB; after the losses from holes are considered, the RCS of reflector will still be around 17.7 dB, equivalent to 60 m^2; for the bigger one, the attenuated RCS will be around 27.6 dB, equivalent to nearly 600 m^2. If the background RCS is low enough, the reflector can still be identified easily for its significant RCS value.

2.5. The Signal-to-Clutter Ratio of Corner Reflector. The corner reflector to be used in the experiment should maximize the RCS or at least the signal-to-clutter ratio (SCR) of the target to allow accurate phase measurements, while keeping the weight and the size as small as possible. SCR is the ratio

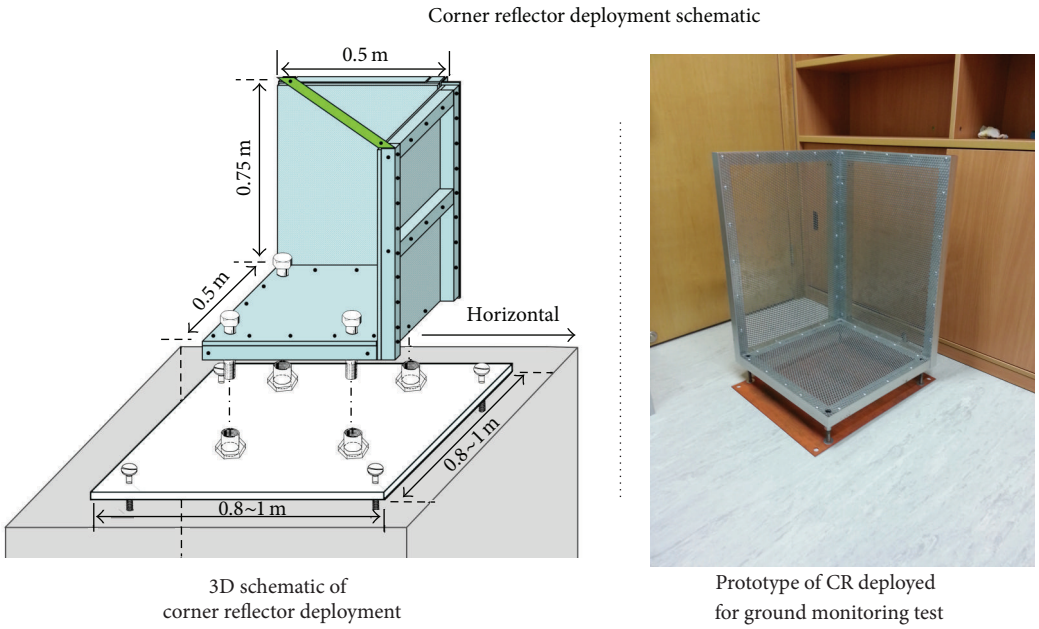

Figure 1: Schematic of corner reflector deployment.

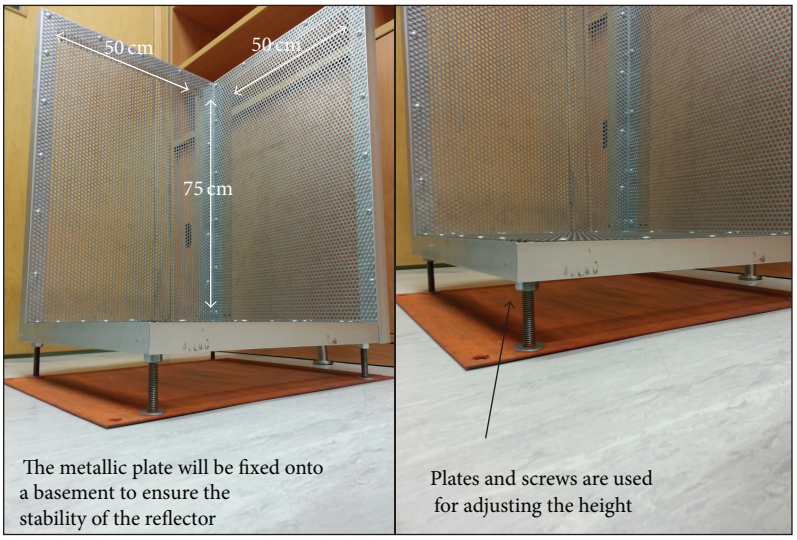

Figure 2: The picture of the reflector.

Table 1: RCSs of the most common reflectors (where a is the side length, and λ is the wavelength).

Types of canonical reflectors	Maximum RCS (m^2)
Triangular trihedral	$4\pi a^4/3\lambda^2$
Rectangular dihedral	$8\pi a^4/\lambda^2$
Square trihedral	$12\pi a^4/\lambda^2$
Circular (quarter disc) trihedral	$15.6\pi a^4/\lambda^2$

between the RCS of the reflector and that of the background scenario and is directly related to the dispersion of the phase values. For high SCR values, the relationship between SCR, phase noise, and the dispersion of the displacement measurements along the satellite line of sight (LOS) can be approximated as follows [19]:

$$\sigma_{\mathrm{LOS}} = \frac{\lambda}{4\pi} \cdot \sigma_{\phi} \approx \frac{\lambda}{4\pi} \cdot \sqrt{\frac{1}{2 \cdot \mathrm{SCR}}},$$
$$\mathrm{SCR} = \frac{\mathrm{RCS}_{\mathrm{corner}}}{\mathrm{RCS}_{\mathrm{background}}} = \frac{A^2_{\mathrm{corner}}}{A^2_{\mathrm{background}}}, \quad (2)$$

where A is the amplitude of the targets. For example, a design requirement on the SCR of 100 (20 dB) corresponds to a dispersion of the displacement measurements in LOS direction of about 0.17 mm at X-band, guaranteeing a theoretical

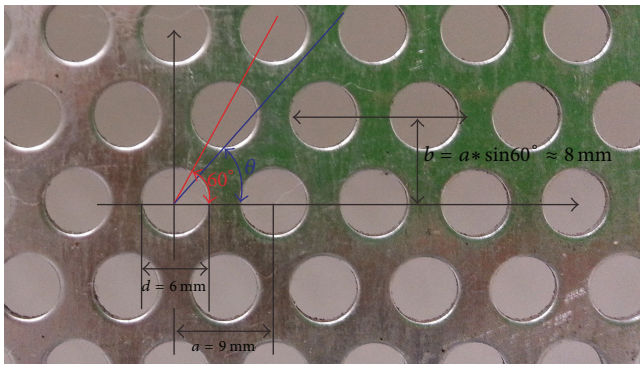

Figure 3: The prototype of the holed plate and the parameters of holes and relative positions.

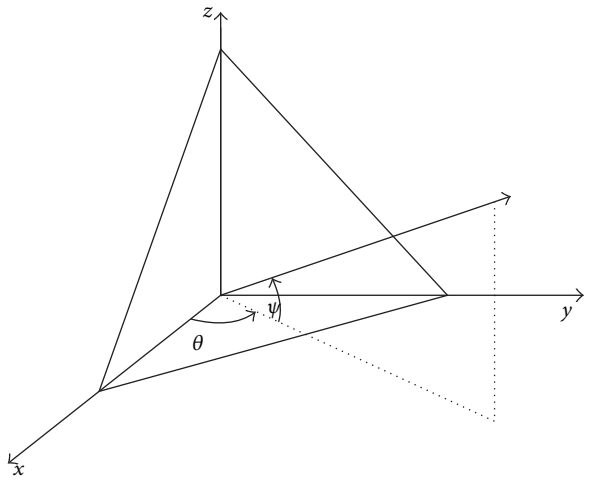

Figure 4: The azimuth angle (θ) and off-nadir angle (Ψ) defined for a corner reflector.

submillimetric dispersion. Naturally, in order to gain a high SCR value and thus a submillimetric dispersion, the CRs should be deployed and placed with low noise value.

2.6. The Installation of Corner Reflector. In order to gain a maximum RCS, the corner reflector should be installed on a horizontal plate and the direction of the reflectors should be set along LOS in order to gain the maximum RCS. If the direction deviates from the LOS direction or tilts slightly, the RCS value would decrease considering the different shape and size of the corners.

Figure 5 plots contours of constant RCS as a function of azimuth and off-nadir angles for a rectangular trihedral reflector with sizes of 0.5 m ∗ 0.5 m ∗ 1 m. The azimuth and off-nadir angle for x-axis and y-axis correspond to θ and Ψ in Figure 4. It is noted that the −3 dB width of the trihedral response spans nearly 20 degrees in azimuth and 20 degrees in off-nadir. This means that the reflector can tolerate a rather high angle excursion without losing much RCS.

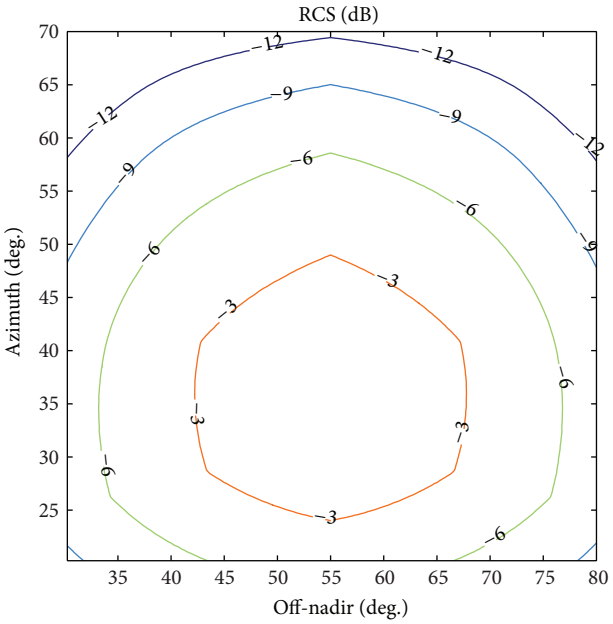

Figure 5: Contours of constant relative RCS for rectangular trihedral corner reflector.

2.7. The Bending of Corner's Plate. The most possible influencing factors that could bias the result are precipitation and bending plates. The former one can be excluded since the holed plate is applied to the test, but still we should consider the curved surfaces that would generate possible delays.

A possible phenomenon that may bend metallic plates is the thermal expansion. However, the calculation reveals that considering the trihedral with mentioned size, the thermal expansion is only able to result in an expansion of 0.1 mm level, thus not very likely to introduce significant bias to our monitoring experiments.

3. On-Site Test for Corner Reflectors

3.1. The Comparison between Two Cubic Trihedrals of Different Sizes. As part of the test, two different sizes of rectangular trihedral corner reflectors, the bigger one being exactly twice the size of the small one, were designed and tested for the experiment to evaluate which one is more applicable. The two prototypes of holed-plated reflectors with sizes of 0.5 m ∗ 0.5 m ∗ 1 m and 1 m ∗ 1 m ∗ 1.5 m have been tested in a football pitch in Hong Kong, and the SAR images are shown in Figure 6. From the images, we can see that with a relative low noise background, the reflectors can be easily identified on SAR images despite the holes. For the bigger reflector, the amplitude is even large enough to generate a star-like graph on SAR image.

The amplitude of two reflectors is compared and shown in Figures 7 and 8. According to Table 1, RCS of the bigger reflector should be 16 times bigger than the smaller one. Meanwhile, in correspondence to the pointwise target k, by means of the calibration constant K_{cal}, we can evaluate the

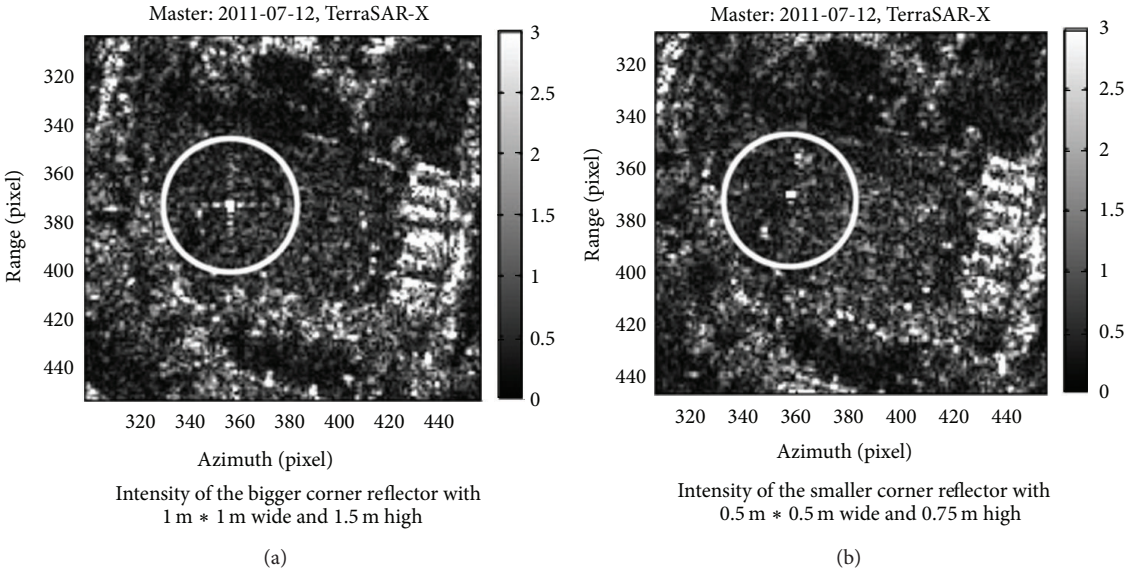

Figure 6: The intensity of two different sizes of reflectors with the same size of holes on the plate. The reflectors are deployed in a football pitch that has a very low noise background, and the signal of the reflector is evident.

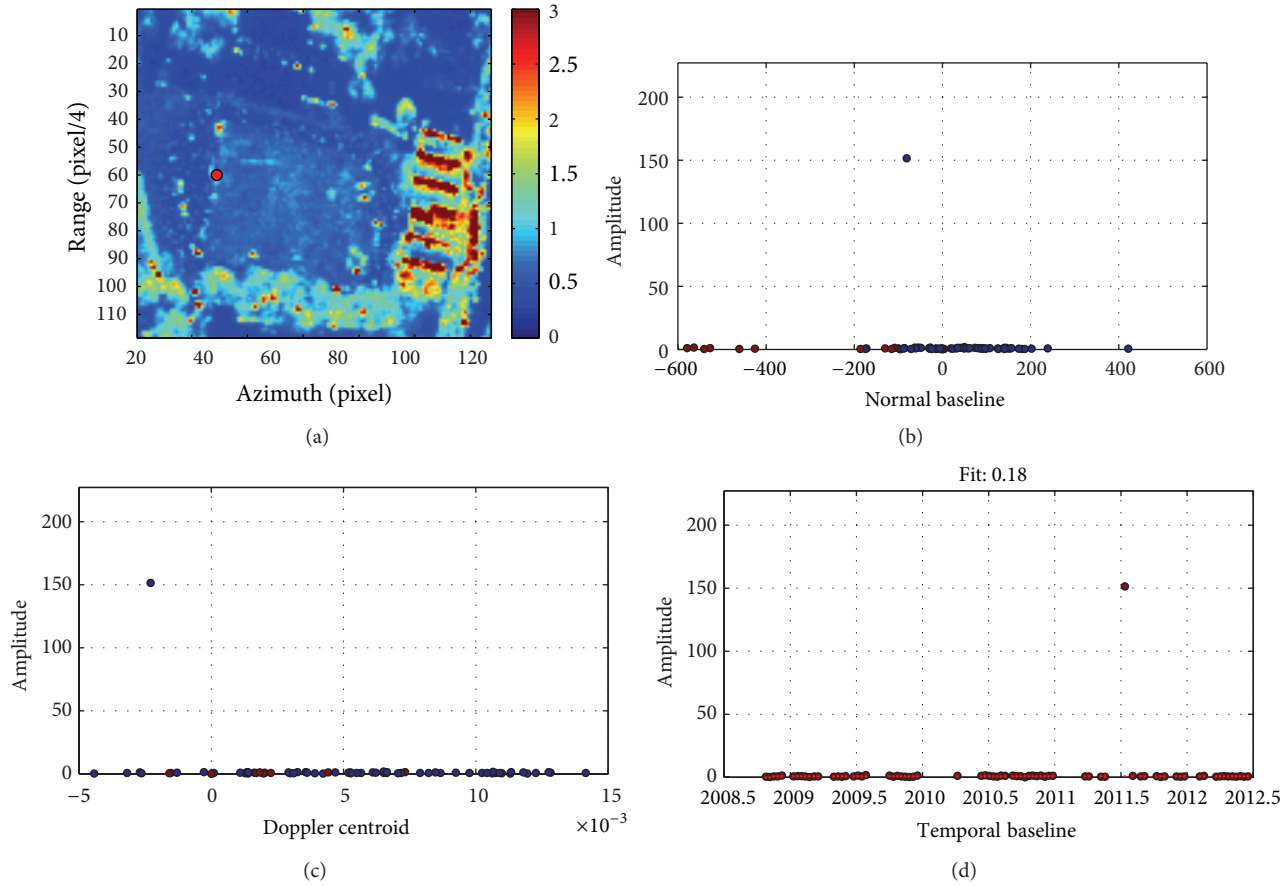

Figure 7: Amplitude Analysis of the bigger corner reflector. (a) shows the location of the reflector; (d) shows the amplitude time series of the location. The one outlined in the amplitude time series indicates the deployment and test of the reflector.

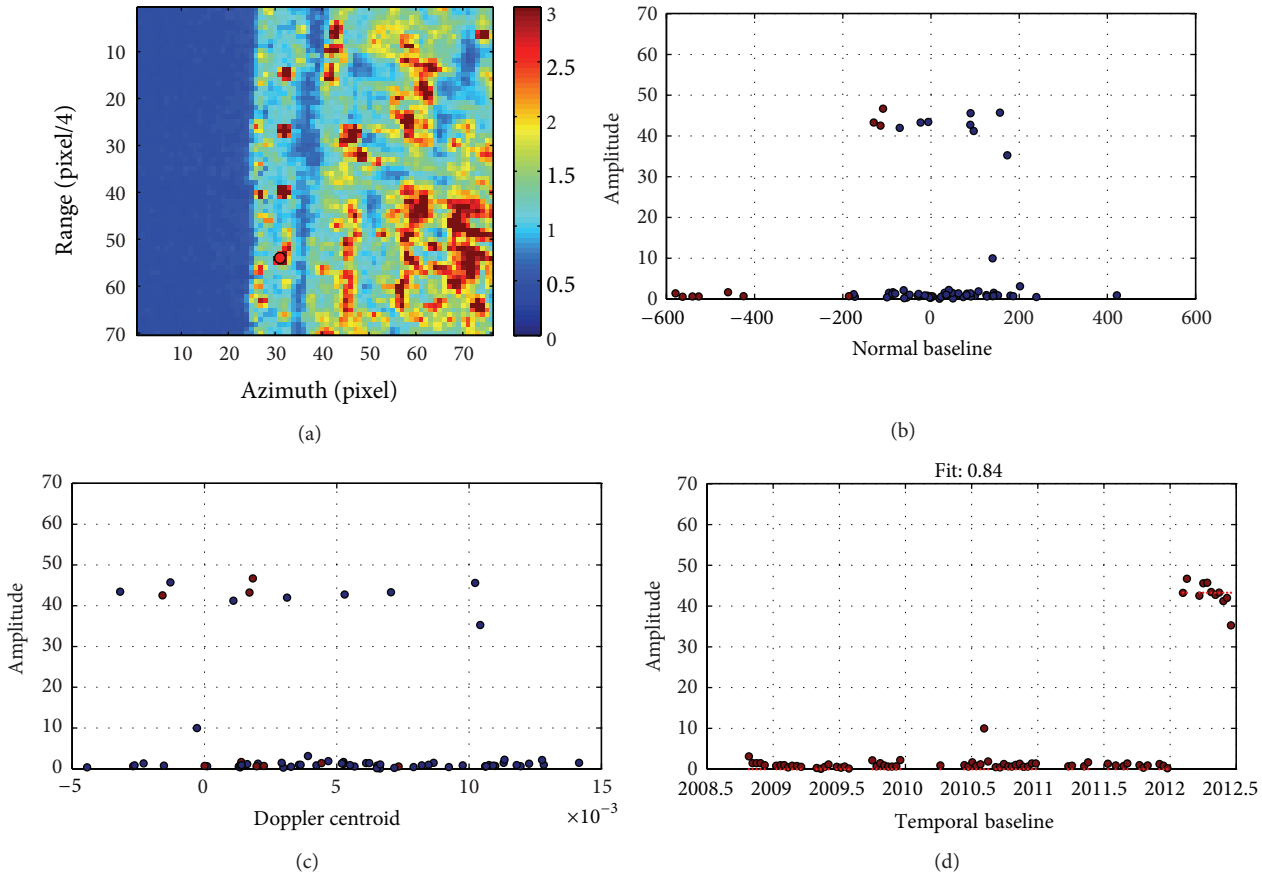

Figure 8: Amplitude analysis of the smaller corner reflector. (a) shows the location of the reflector; (d) shows the amplitude time series of the location. The amplitude leap indicates the deployment of reflectors.

Figure 9: (a) The location of CRs in optical image displayed in Google Earth. The location is near the sea that is identical for its low intensity in RADAR images. (b) The location and intensity of the four CRs on TSX images. From the images, we can see that the background radiation in that area is very low, and the intensity of CRs is considerably high.

relationship between amplitude and RCS by the following equation:

$$\mathrm{RCS}_k = \mathrm{Amplitude}_k^2 \times K_{\mathrm{cal}}, \quad (3)$$

where K_{cal} is the calibration constant [20]; thus the amplitude of the bigger RCS should be theoretically 4 times the amplitude of the smaller one. In this experiment, as shown in Figures 7 and 8, the amplitude of the bigger one is around 3.5 times the smaller one, which is rather close to the theoretical value a rough estimation.

Generally speaking, since the mechanical stability and accuracy of the shifts to the reflector must be precisely controlled to millimetric level, both the size and weight of the reflector should be kept to a certain limit. In other words, the shape and size of reflector must seek thier balance between a good RCS value and an applicable size. By looking into the amplitude time series of the reflectors in Figures 7 and 8, we can see that both reflectors are showing a very good SNR and identifiable amplitude change. However when considering the size and weight of the reflectors, the smaller one should be preferred for its convenience in carrying and deployment.

3.2. The Deployment of Corner Reflector. An ideal place for placing the reflectors is an area that presents a low background radiation to facilitate identifying the CR and to guarantee good phase stability. In addition, in order to demonstrate the PSInSAR capability of detecting millimetric changes with CR, it is suggested to place all the CRs within a certain distance, in order to avoid possible unexpected relative motions and to keep the atmospheric noise as limited as possible. In general, this distance should not exceed 200 meters [21]. For example, as shown in Figure 9, we deployed four CRs in an area where the background radiation is considerably low. The four CRs are within a range of 200 meters so that the atmospheric noise is kept to a low level. One of them is selected as the reference target for the process, which means that it will stay stable in all the time.

3.3. The Validation Test of Corner Reflector. In order to evaluate the performance of this type of CR, a validation test is carried out in urban area in Hong Kong. As shown in Figure 9, four CRs are deployed in an area with low background scattering. The reflector toward far west is set to be the reference scatterer and was kept stable, while the others are being manually lifted. For the estimation of corresponding PSInSAR movement of each CR, totally 11 scenes from January 2012 to June 2012 of TerraSAR-X and TanDEM-X data have been applied for analysis. The TSX and TDX satellites for generating the images process an active-phases array X-band SAR antenna with a wavelength of 31 mm and frequency of 9.6 GHz, with a resolution of up to 1 meter. The minimum interval between the two consequent acquisitions is 11 days. The TSX sensor acquires images over Hong Kong at about 6:25 PM, along an ascending orbit (from north to south, edging slightly westward) and it is right-looking, with an incidence angle of approximately 37 degrees.

To analyze the performance of PSInSAR technique, the estimated PSInSAR-derived displacements and values measured by ground survey were being compared, and a linear regression is conducted for the purpose of analyzing the deviation between the two measurements. The linear correlation coefficient of the regression is higher than 0.99, stating univocally the linear correlation between the displacements detected by InSAR and by the leveling survey. The root mean square error (RMSE) is around 0.85 mm, lower than 1 mm. In other words, the outcome of the analysis is slightly better than the best result that could be expected from such an analysis, revealing that InSAR can definitely reach the same accuracy of optical leveling and may overtake it.

4. Conclusion

In this paper, we discussed the design and experiments on different types and sizes of corner reflectors and brought up a small-size rectangular trihedral reflector. We concluded the great superiority of this type for deploying and estimating the difference between InSAR and ground truth data, by which the PSInSAR estimated deformation results can be easily validated and applied. The type of corner reflector has demonstrated its ability and potential in PSInSAR analysis, perfectly balancing the mobility, stability, and precision, showing an accuracy of less than 1 mm and thus making a good reference as a corner reflector prototype.

Acknowledgments

The TerraSAR-X data used in this project have been provided by Infoterra Germany, through the cooperation with Ralf Duering, Beijing. This work was partially supported by the Research Grants Council (RGC), General Research Fund (GRF) (Project Reference no. 415911) of HKSAR, and Direct Grant Funded Project (Reference no. 2021130).

References

[1] J. C. Curlander and R. N. McDonough, *Synthetic Aperture Radar: Systems and Signal Processing*, John Wiley & Sons, New York, NY, USA, 1991.

[2] R. Gens and J. L. van Genderen, "SAR interferometry—issues, techniques, applications," *International Journal of Remote Sensing*, vol. 17, no. 10, pp. 1803–1835, 1996.

[3] F. Amelung, D. L. Galloway, J. W. Bell, H. A. Zebker, and R. J. Laczniak, "Sensing the ups and downs of Las Vegas: InSAR reveals structural control of land subsidence and aquifer-system deformation," *Geology*, vol. 27, no. 6, pp. 483–486, 1999.

[4] H. A. Zebker and J. Villasenor, "Decorrelation in interferometric radar echoes," *IEEE Transactions on Geoscience and Remote Sensing*, vol. 30, no. 5, pp. 950–959, 1992.

[5] H. A. Zebker, P. A. Rosen, and S. Hensley, "Atmospheric effects in interferometric synthetic aperture radar surface deformation and topographic maps," *Journal of Geophysical Research: Solid Earth*, vol. 102, no. 4, pp. 7547–7563, 1997.

[6] A. Ferretti, C. Prati, and F. Rocca, "Permanent scatterers in SAR interferometry," *IEEE TGARS*, vol. 39, no. 1, 2001.

[7] A. Ferretti, G. Savio, R. Barzaghi et al., "Submillimeter accuracy of InSAR time series: experimental validation," *IEEE Transactions on Geoscience and Remote Sensing*, vol. 45, no. 5, pp. 1142–1153, 2007.

[8] A. H.-M. Ng, L. Ge, X. Li, and K. Zhang, "Monitoring ground deformation in Beijing, China with persistent scatterer SAR interferometry," *Journal of Geodesy*, vol. 86, no. 6, pp. 375–392, 2012.

[9] Q. Zhao, H. Lin, W. Gao, H. A. Zebker, A. Chen, and K. Yeung, "InSAR detection of residual settlement of an ocean reclamation engineering project: a case study of Hong Kong International Airport," *Journal of Oceanography*, vol. 67, no. 4, pp. 415–426, 2011.

[10] G. Herreraa, R. Tomás, J. M. Lopez-Sanchez et al., "Validation and comparison of Advanced Differential Interferometry Techniques: murcia metropolitan area case study," *ISPRS Journal of Photogrammetry and Remote Sensing*, vol. 64, no. 5, pp. 501–512, 2009.

[11] B. C. Brock and A. W. Doerry, "Radar cross section of triangular trihedral reflector with extended bottom plate," 2009.

[12] E. F. Knott, "RCS reduction of dihedral corners," *IEEE Transactions on Antennas and Propagation*, vol. 25, no. 3, pp. 406–409, 1977.

[13] S. Y. Wang and S. K. Jeng, "Compact RCS formula for a dihedral corner reflector at arbitrary aspect angles," *IEEE Transactions on Antennas and Propagation*, vol. 46, no. 7, pp. 1112–1113, 1998.

[14] K. Hayashi, R. Sato, Y. Yamaguchi, and H. Yamada, "Polarimetric scattering analysis for a finite dihedral corner reflector," *IEICE Transactions on Communications*, vol. E89-B, no. 1, pp. 191–195, 2006.

[15] P. Corona, A. de Bonitatubus, G. Ferrara, and C. Gennarelli, "A very accurate model for backscattering by right angled dihedral corners," in *Proceedings of the IEEE Antennas and Propagation Society International Symposium*, vol. 4, pp. 1734–1737, May 1990.

[16] X.-J. Shan, J.-Y. Yin, D.-L. Yu, C.-F. Li, J.-J. Zhao, and G.-F. Zhang, "Analysis of artificial corner reflector"s radar cross section: a physical optics perspective," *Arabian Journal of Geosciences*, 2012.

[17] T. Y. Otoshi, "Study of microwave leakage through perforated flat plates," *IEEE Transactions on Microwave Theory and Techniques*, vol. 20, no. 3, pp. 235–236, 1972.

[18] A. Parizzi, D. Perissin, C. Prati, and F. Rocca, "Artificial scatterers in SAR interferometry," in *Proceedings of Dragon Symposium*, Santorini, Greece, June-July 2005.

[19] G. Ketelaar, P. Marinkovic, and R. Hanssen, "Validation of point scatterer phase statistics in multi-pass InSAR," in *Proceedings of CEOS SAR Workshop*, Ulm, Germany, May 2004.

[20] D. Perissin and A. Ferretti, "Urban-target recognition by means of repeated spaceborne SAR images," *IEEE Transactions on Geoscience and Remote Sensing*, vol. 45, no. 12, pp. 4043–4058, 2007.

[21] P. Marinkovic, G. Ketelaar, F. van Leijen, and R. Hanssen, "InSAR quality control—analysis of five years of corner reflector time series," in *Proceedings of the 5th International Workshop on ERS/Envisat SAR Interferometry (FRINGE '07)*, Frascati, Italy, November 2007.